



Published in final edited form as:

J Bone Miner Res. 2020 December ; 35(12): 2432–2443. doi:10.1002/jbmr.4142.

LACTATE DEHYDROGENASE INHIBITION WITH OXAMATE EXERTS BONE ANABOLIC EFFECT

Alex M. Hollenberg¹, Charles O. Smith¹, Laura C. Shum¹, Hani Awad¹, Roman A. Eliseev^{1,*}

¹Center for Musculoskeletal Research, University of Rochester School of Medicine & Dentistry, Rochester, NY

Abstract

Cellular bioenergetics is a promising new therapeutic target in aging, cancer, and diabetes as these pathologies are characterized by a shift from oxidative to glycolytic metabolism. We have previously reported such glycolytic shift in aged bone as a major contributor to bone loss in mice. We and others also demonstrated the importance of oxidative phosphorylation (OxPhos) for osteoblast differentiation. It is therefore reasonable to propose that stimulation of OxPhos will have bone anabolic effect. One strategy widely used in cancer research to stimulate OxPhos is inhibition of glycolysis. In this work, we aimed to evaluate the safety and efficacy of pharmacological inhibition of glycolysis to stimulate OxPhos and promote osteoblast bone-forming function and bone anabolism. We tested a range of glycolytic inhibitors including 2-deoxyglucose, dichloroacetate, 3-bromopyruvate, and oxamate. Of all the studied inhibitors, only lactate dehydrogenase (LDH) inhibitor, oxamate, did not show any toxicity in either undifferentiated osteoprogenitors or osteoinduced cells *in vitro*. Oxamate stimulated both OxPhos and osteoblast differentiation in osteoprogenitors. *In vivo*, oxamate improved bone mineral density, cortical bone architecture, and bone biomechanical strength in both young and aged C57BL/6J male mice. Oxamate also increased bone formation by osteoblasts without affecting bone resorption. In sum, our work provided a proof of concept for the use of anti-glycolytic strategies in bone and identified a small molecule LDH inhibitor, oxamate, as a safe and efficient bone anabolic agent.

Keywords

Bone; osteoblast; lactate dehydrogenase; glycolysis; mitochondria; oxamate

INTRODUCTION

Bone marrow stromal cells (BMSCs) are somatic multipotent progenitors of the mesenchymal lineage. These cells are characterized by their capacity to differentiate into bone-forming osteoblasts, cartilage producing chondrocytes, and fat storing adipocytes.⁽¹⁾

*To Whom The Correspondence Should Be Addressed: Roman Eliseev, MD, PhD, University of Rochester Medical Center, 601 Elmwood Ave, Rm 1-8541, Rochester, NY 14642, Tel: 585-276-3396, roman_eliseev@urmc.rochester.edu.

AUTHOR CONTRIBUTIONS

Conceptualization, R.A.E.; Investigation, A.H., L.C.S., and C.O.S.; Writing & Editing, A.H., C.O.S., H.A. and R.A.E; Supervision, H.A. & R.A.E.

Bone stability is maintained by the equilibrium between osteoblasts and bone resorbing osteoclasts of a monocyte/macrophage cell lineage.⁽²⁻⁴⁾ Disruption of this balance in pathologies including osteoporosis, diabetes, cancer, and metabolic disorders results in a decline of bone quality, typically manifesting as an increase in fracture risk.⁽⁵⁻⁷⁾

Aging is a multifaceted phenomenon characterized by decreased function at the tissue, cellular, and organelle level. Increased fracture risk is a common characteristic in the elderly as a result of reduced bone mass and loss of mineral density as resorptive processes outpace osteogenesis.^(8,9) The progression of an aged phenotype is marked by decreased hormonal stimulation and increased oxidative stress, among other age associated factors. Intriguingly, many such factors converge on the mitochondria and result in disruption of mitochondrial function.⁽¹⁰⁾ Decreased mitochondrial membrane integrity as a result of damage leads to decreased oxidative phosphorylation (OxPhos) capacity and disruptions in biosynthesis pathways and ion transport.⁽¹¹⁻¹⁷⁾ Dysfunctions in osteoprogenitor differentiation into mature osteoblasts contribute to the loss of equilibrium in bone homeostasis.⁽¹⁸⁾ Cellular metabolism of stem and progenitor cells is a rapidly growing area of interest. The view that stem cells are metabolically obligate anaerobic has been expanded to reveal novel roles and requirements for the mitochondria. In many cases, differentiation of stem cells, including BMSCs, coincides with upregulation of mitochondrial respiration,⁽¹⁹⁻²¹⁾ however the physiologic relevance of such transitions remains incompletely understood.⁽²²⁻²⁴⁾ Targeting mitochondria-derived oxidative stress as a secondary pathogenic factor in aging associated with bone loss has recently come into focus as a potential therapeutic.^(19,21,22) However the impact of mitochondria-targeted therapies on bone have not been thoroughly studied.

There are numerous similarities between stem cells and cancer cell behavior including their reliance on glycolysis.⁽²⁵⁾ Changes in metabolic programs have been well documented in the cancer field,^(26,27) and anti-glycolytic agents have been successfully employed in cancer research.⁽²⁸⁻³¹⁾ By shifting energy metabolism from glycolysis to OxPhos, these agents promote differentiation signaling in cancer cells. The same strategy may be applied to stem and progenitor cells in order to stimulate their differentiation, e.g. to differentiation of osteoprogenitors into OBs needed for bone anabolism.

Herein we used a panel of glycolytic inhibitors: 2-deoxyglucose (2DG), dichloroacetate (DCA), 3-bromopyruvate (3-BP), and sodium oxamate (OXA), and examined their safety *in vitro* and *in vivo*, ability to shift cell bioenergetics from glycolysis to OxPhos in osteoprogenitors, and ability to impact osteogenesis and bone anabolism.

MATERIALS AND METHODS

Materials

Chemicals and reagents were acquired from Sigma unless otherwise specified.

Cell culture and osteoblast differentiation

C3H10T1/2 cells were purchased from ATCC. Human BMSCs were from Lonza. These cells have been used extensively in the field and in our previous works.^(19,32) Both types of cells were grown in DMEM/low-glucose (5 mM) medium supplemented with 1 mM

glutamine, 10% fetal bovine serum, and 1% penicillin/streptomycin mixture (Gibco). For all experiments, cells at passages 5 to 10 were used as recommended by the distributor. Cells were osteogenically induced by treating with 50 µg/ml ascorbic acid and 2 mM β-glycerol phosphate for 14 days. To confirm osteoinduction, cells were stained with alkaline phosphatase-specific stain (ALP) and Aizarin Red mineralization stain or collected for RNA isolation and analysis of osteoblast-specific gene expression using real-time RT-PCR as described below. Three different batches of cells were used to achieve three biological replicates. For each assay/condition we used two wells as technical replicates.

Cell viability assay

To determine cell viability after treatment with various glycolytic inhibitors, a Calcein AM staining was performed. Cells were plated on a black-wall clear-bottom 96-well plate and after 24 h incubation, treated with phosphate-buffered saline (PBS) as a vehicle control or various indicated doses of 2DG, DCA, 3-BP, or OXA for 48 h and then stained with Calcein AM at 1 µM for 30 min. Calcein fluorescent signal was detected using BioTek plate reader. To achieve multiple biological replicates, three different batches of cells were used to seed three plates. Each condition was repeated in four wells (four technical replicates).

Bioenergetic profiling

Oxygen consumption rate (OCR) and extracellular acidification rate (ECAR) were measured using Seahorse XF96 (Seahorse Bioscience). OCR is the measure of OxPhos activity and ECAR is the measure of glycolytic activity. Undifferentiated and osteoinduced cells were plated on Seahorse 96-well plates at a density of 15,000 cells/well and assayed after 48 h. Five different plates (biological replicates) were used; and each condition was repeated in multiple wells on one plate (technical replicates). Immediately prior to the experiment, medium was replaced with DMEM-XF media (unbuffered DMEM base added with 5 mM glucose, 1 mM glutamine, 1% serum, and 1 mM OXA or PBS, pH 7.4). A baseline OCR and ECAR measurement was taken, and then an inhibitory analysis was performed. Inhibitors included oligomycin (Olig) at 1 µM, FCCP at 0.5 µM, and a mixture of antimycin A and rotenone (AntA/Rot) both at 1 µM. Key mitochondrial metabolic parameters were calculated from the resulting OCR measures including: basal, ATP-linked, proton leak, maximal respiration, and spare respiratory capacity. Basal glycolytic rate was calculated from $ECAR_{pre-Olig}$. The calculations were performed as described in our previous work.⁽¹⁹⁾ Briefly, basal OCR is the difference between $OCR_{pre-Olig}$ and $OCR_{post-AntA/Rot}$; ATP-linked OCR is the difference between $OCR_{pre-Olig}$ and $OCR_{post-Olig}$; Proton Leak is the difference between $OCR_{post-Olig}$ and $OCR_{post-AntA/Rot}$; Max Respiration is the difference between $OCR_{post-FCCP}$ and $OCR_{post-AntA/Rot}$; and Spare Capacity is the difference between $OCR_{post-FCCP}$ and $OCR_{pre-Olig}$.

Real-time reverse transcriptase polymerase chain reaction

Total RNA was isolated using the RNAeasy kit (Qiagen) and reverse transcribed into cDNA using iScript cDNA synthesis kit (Bio-Rad). Real-time RT-PCR was performed in the RotorGene system (Qiagen) using SYBR Green (Quanta). The expression of genes of interest was normalized to the expression of β-2-microglobulin gene. The following primer pairs were used: mouse *Runx2* (5'-CCG GGA ATG ATG AGA ACT AC-3' and 5'-CCG

TCC ACT GTC ACT TTA ATA-3'), *Alp* (5'-CAT GTA CCC GAA GAA CAG AAC-3' and 5'-GGG CTC AAA GAG ACC TAA GA-3') and *B2m* (5'-AAT GGG AAG CCG AAC ATA C-3' and 5'-CCA TAC TGG CAT GCT TAA CT-3') and human *Runx2* (5'-TCC GGA ATG CCT CTG CTG TTA TGA-3' and 5'-ACT GAG GCG GTC AGA GAA CAA ACT-3'), *ALP* (5'-TGC AGT ACG AGC TGA ACA GGA ACA-3' and 5'-TCC ACC AAA TGT GAA GAC GTG GGA-3') and *B2M* (5'-CAG CAA GGA GTC TTT CTA-3' and 5'-ACA TGT CTC GAT CCC ACT TAA-3').

Animal care and treatment

Animal husbandry and experiments were performed in accordance with the Division of Laboratory Animal Medicine, University of Rochester, state and federal law, and National Institutes of Health policies. University of Rochester Institutional Animal Care and Use Committee specifically approved all animal work. Wild type C57BL/6J breeders were purchased from Jackson Laboratories and bred in house. Eight-week-old or 18 month-old male C57BL/6J mice were intraperitoneally injected with 100 mg/kg OXA or PBS twice per week. After eight weeks of treatment, whole-body and toxicity measures were conducted. Body weight was measured in grams. Blood samples were collected and serum alanine aminotransferase (ALT) and creatinine were measured using ALT assay kit and Creatinine assay kit (Cayman Chemicals) respectively, per manufacturer instructions. Body fat percentage, lean mass, and bone mineral density (BMD) were measured by Dual Energy X-ray Absorptiometry (DEXA) using LUNAR PIXImus 2 scanner.

Metabolomics

Mice treated with either OXA or PBS were euthanized and their hind limbs dissected according to previous methods.⁽¹⁷⁾ Briefly, the tibia and femurs were cleaned of soft tissue and bone marrow and then flash frozen in liquid nitrogen. When all the samples were collected, bones were ground to powder using ceramic mortar placed on dry ice and pestle and the dry powder was transferred to 80% MeOH at -80°C. Metabolites were extracted using methanol extraction as previously described.⁽³³⁾ Samples were vortexed and spun in a table-top centrifuge at 13,000 RPM for 10 minutes; then the supernatant was transferred to a 50 mL conical tube and evaporated under a nitrogen gas stream. The pellet was used to calculate protein content for normalization. After evaporation, samples were resuspended in 50% MeOH and analyzed by LC-MS/MS to measure steady state abundance of metabolites. Data for each run were median-normalized. Overall, 85 metabolites were identified of which 6 (7%) were removed due to insufficient replicates yielding 790 theoretical individual data points (79 x N=5, x 2 groups). Metabolomic data were analyzed using Metaboanalyst software.⁽³⁴⁾

Bone micro-CT

After whole body measures and blood sample collection, mice treated with either OXA or PBS were euthanized. The femurs, tibiae, and spines were isolated and cleaned of adherent soft tissue. The right femurs were used for biomechanical torsion testing. The left femurs, tibiae, and spines were placed in 10% neutral buffered formalin (NBF) for fixation. After 72 h fixation, the bones were imaged using a VivaCT 40 tomograph (Scanco Medical). A calibrating phantom was used to standardize radiodensities for each scan. Volume

quantification was performed using Scanco analysis software. For each right femur and lumbar spinal vertebrae (L3) sample, bone vs total volume (BV/TV), trabecular number (Tb N), trabecular thickness (Tb Th), trabecular bone mineral density (Tb BMD), cortical thickness (Cort Th), cortical area (Cort Area), marrow area, polar moment of inertia (PMOI), and cortical bone mineral density (Cort BMD) were measured. After micro-CT scans, bone were further processed for paraffin embedding to obtain formalin-fixed paraffin embedded (FFPE) blocks.

Dynamic bone histomorphometry

Calcein double labeling was performed to determine the extent of new bone formation with OXA treatment. OXA and PBS treated mice were intraperitoneally injected with calcein (10 mg/kg) 10 and 5 days prior to sacrifice. After sacrifice, right femoral bones were isolated, cleaned of soft tissue, and processed for frozen sectioning. Calcein bands were viewed using a fluorescence Axioscope 40 microscope (Zeiss). Bone formation rate (BFR) was calculated as follows: $BFR = MAR \times (MS/BS)$ where $MAR = Ir.L.Th/Ir.L.t.$ and $MS = (dLS + sLS/2)/BS$ (MAR, mineral apposition rate; BS, bone surface; dLS, double labelled surface; sLS, single labelled surface; Ir.L.Th, distance between labels; and Ir.L.t, time between labels).

Bone resorption assay

To assess osteoclast activity, FFPE femur sections were stained for tartrate-resistant acid phosphatase (TRAP) as described in our previous work.⁽¹⁷⁾ Slides were scanned in an Olympus VSL20 whole slide imager. TRAP positive osteoclasts were detected with Visiopharm automated histomorphometry software that calculated osteoclast area per total bone area.

Bone Biomechanical testing

Biomechanical properties of mice after treatment with OXA or PBS were assessed via femoral torsion testing. Bone samples were collected, cleaned from soft tissue, wrapped in PBS-soaked gauze and stored in paraffin-sealed tubes to prevent drying in -80°C until the day of testing. After thawing, bone ends were secured on holders with bone cement (DePuy Orthopaedics) and tested using an EnduraTec system (Bose) at a displacement rate of $1^{\circ}/\text{s}$ until failure. The data were plotted against rotational deformation to determine the torsional rigidity, maximum torque, rotation at maximum torque, and energy to yield.

Statistical analysis

All statistical analyses were performed in GraphPad Prism 8.0. Mean values and standard deviations were calculated. A one-way analysis of variance (ANOVA) was used to compare > 2 variables. An unpaired *t*-test was used when 2 variables were compared. The significance level was set at $p < 0.05$. In each of the *in vitro* assays, we used multiple technical replicates to achieve one biological replicate.

RESULTS

Effect of various anti-glycolytic agents on osteoprogenitors

To determine whether inhibition of glycolysis leads to compensatory activation of OxPhos and subsequent stimulation of osteoblast differentiation, we utilized a commonly used osteoprogenitor cell line, C3H10T1/2 and tested various glycolytic inhibitors. In our previous publication, we showed that undifferentiated C3H10T1/2 cells are primarily glycolytic, but activate OxPhos during osteoblast differentiation.⁽¹⁹⁾ Since glycolysis may be important for maintenance of undifferentiated cells, we first measured how various glycolytic inhibitors (Fig. 1A) affect viability of undifferentiated C3H10T1/2 cells. For each agent, we tested a range of concentrations based on the previous literature.^(29,30,35) Figure 1B shows that the inhibitors of the early steps of glycolysis, 2DG and 3BP, as well as the inhibitor of the regulator of the last step of glycolysis, DCA, all significantly reduced cell viability after 48h of treatment. However, the inhibitor of lactate dehydrogenase (LDH), OXA, did not cause any toxicity at studied concentrations. To determine OXA safety window in C3H10T1/2 cells *in vitro*, we used higher concentrations of the compound (5, 7.5, and 10 mM). There was no significant decrease in viability at either 5 mM OXA (102% \pm 3%) or 7.5 mM OXA (92% \pm 6%) vs PBS. Moderate but statistically significant reduction of cell viability was only observed at 10 mM OXA (79% \pm 4%, $p < 0.05$ vs PBS-treated controls by *t*-test, $n = 3$). The toxic effect induced by 2DG, 3BP, and DCA was likely due to the undifferentiated cells' requirement for uninterrupted flow of substrates from the first glucose utilization step (HK-dependent) to the last step (pyruvate to Ac-CoA). These compounds work by interrupting such a flow. OXA, on the other hand, is not expected to interrupt the flow but to divert it towards pyruvate oxidation.

Osteoprogenitors, including C3H10T1/2 cells, shift their energy metabolism towards OxPhos during osteoblast differentiation.⁽¹⁹⁾ Therefore, cell sensitivity to metabolic inhibitors and modifiers may change during differentiation. To test whether OXA is safe for differentiated C3H10T1/2 cells, we induced osteoblast differentiation using osteogenic media for 14 days and then treated cells with the indicated concentrations of OXA for 48 h. Figure 1C shows absence of any significant negative effect on viability of osteoinduced C3H10T1/2 cells.

Therefore, LDH inhibitor OXA can be safely used in both osteoprogenitors and differentiated osteoblasts at the studied concentrations *in vitro*.

LDH inhibitor oxamate diverts cell bioenergetics from glycolysis to oxidative phosphorylation

To confirm that OXA at 1 mM can in fact inhibit glycolysis, we performed bioenergetic profiling of both undifferentiated and osteoinduced C3H10T1/2 cells in the presence or absence of OXA at 1 mM using Seahorse XF technology. Figure 2A (left panels) shows that as expected, undifferentiated C3H10T1/2 cells are not very active and their reliance on OxPhos is minimal, as evident from the low basal OCR and moderate responses to metabolic modifiers, including ATP synthase inhibitor oligomycin and uncoupler FCCP. In undifferentiated C3H10T1/2 cells, OXA at 1 mM did not have any effect on OxPhos or basal

glycolysis measured via the ECAR due to lactate production. It did however prevent compensatory activation of glycolysis after inhibition of OxPhos with oligomycin (Fig. 2A, bottom left panel).

In cells that underwent osteoblastic differentiation for 14 days, OxPhos was activated; and responses of both OxPhos and glycolysis to metabolic modifiers were well pronounced (Fig. 2A, right panels). In these osteoinduced cells, OXA treatment led to inhibition of glycolysis and further activation of OxPhos. Figures 2B and 2C show quantitation of changes in OxPhos parameters and glycolysis, respectively. Specifically, basal, ATP-linked, and maximal respiration were all significantly increased while glycolysis was significantly inhibited in OXA-treated osteoinduced cells.

Thus, while OXA at 1 mM has minimal effect on bioenergetics in undifferentiated cells that have low energy demands, it inhibits glycolysis and stimulates OxPhos in osteoinduced cells that have higher energy demands.

LDH inhibition increases osteogenic potential of C3H10T1/2 mouse osteoprogenitors and human BMSCs

We and others have previously reported that stimulation of OxPhos increases osteogenic potential in osteoprogenitors, including C3H10T1/2 cells and human BMSCs.^(19,21,36) To determine whether OXA has pro-osteogenic effects, we assessed markers of osteoblast differentiation in osteoinduced C3H10T1/2 cells treated or not with OXA at 1 mM. Figure 3A shows that C3H10T1/2 cells osteoinduced for 14 days have pronounced alkaline phosphatase (ALP) and Alizarin Red mineralization staining which is further increased in the presence of OXA (Fig. 3A). Osteoblast-specific genes, *Runx2* and *Alp*, were upregulated to a significantly higher extent in the presence of OXA compared to PBS-treated controls, as was measured via real-time RT-PCR (Fig. 3B and C).

To validate this effect in primary cells with osteogenic potential, we used human BMSCs. Figure 3D – F shows that hBMSCs osteoinduced for 14 days in the presence of OXA have significantly higher levels of ALP and Alizarin Red staining and *RUNX2* and *ALP* expression when compared to PBS-treated osteoinduced cells.

These data indicate that LDH inhibition with OXA not only stimulates OxPhos, but also increases osteogenic potential of osteoprogenitors.

Mice treated with LDH inhibitor oxamate have increased bone mineral density without any signs of toxicity

Since our goal was to elucidate a therapeutic potential of glycolytic inhibitors in bone, we studied the effect of OXA in mice *in vivo*. Having observed a significant pro-osteogenic effect of OXA *in vitro*, we expected that OXA would stimulate bone formation leading to bone anabolic effects in mice. We therefore treated 8-week-old male mice q2wk with 100 mg/kg OXA for 8 weeks and then analyzed mouse bones (Fig. 4A). The dose was chosen based on previous studies performed in mice.^(31,37) As this was a proof-of-concept experiment, we chose male mice only to avoid potential and well-documented effects of estrogen on mitochondria and OxPhos that could mask the effect of OXA in female mice.

(8,38–41) Our rationale for using 8-week-old mice here was that if we see a bone anabolic effect in these young mice that are not yet expected to have any metabolic disturbances, we are much more likely to see the effect in aged mice that have a glycolytic shift in bone tissue according to our previous work.⁽¹⁷⁾ This will be a strong argument for pursuing expensive and time-consuming aging studies involving different ages and both sexes.

First, we assessed OXA treatment safety by measuring mouse weights, liver toxicity (serum ALT levels), and kidney toxicity (serum creatinine levels). Figure 4B – D shows that no signs of OXA toxicity was detected in treated mice; neither body weight nor serum ALT was significantly changed; and serum creatinine was not increased, but even decreased. We then measured whole body composition via DEXA and found significantly decreased body fat percentage (Fig. 4E) and increased lean mass and BMD (Fig. 4F & G).

These studies indicate that LDH inhibitor OXA increases BMD and reduces fat without causing toxicity in mice.

LDH inhibition with oxamate does not cause significant shifts in steady-state metabolites in bone

Inhibition of LDH by OXA has the potential to change cellular energy metabolism. We currently have limited means of measuring cellular energy metabolism *in vivo*. Data obtained by analyzing cells isolated from a tissue cannot be easily extrapolated to the *in vivo* situation. Cell isolation usually involves mechanical disruption and/or enzymatic processing that can dramatically change cellular energy metabolism.⁽⁴²⁾ Metabolomics of rapidly processed and flash frozen whole tissue is currently the only available method of detecting bioenergetic changes *in vivo*. The method is limited to measuring steady-state levels of small metabolites. We therefore asked whether we could observe a shift in the steady-state metabolite levels in OXA-treated bone. Using OXA- or control PBS-treated mice, we performed metabolite extraction from shafts of tibia and femurs. These samples were cleaned of soft tissue and periosteum and contained bone associated cells, i.e. osteoblasts and osteocytes likely with insignificant contribution from other types of cells, such as osteoclasts etc. We performed a targeted metabolomics screen focusing on central metabolic pathways (glycolysis, TCA cycle, pentose-phosphate pathway, amino acid and ketone synthesis and degradation), nucleotide content, and redox markers (Supplementary Fig. S1). Our analysis revealed that while OXA did not produce a significant change in steady-state metabolite content in whole bone samples (Supplementary Table S1), there was a trend towards increased metabolites in glycolysis, pyruvate, Acetyl-CoA, and redox pathway, which could suggest increased metabolic flux through mitochondria (Supplementary Fig. S2). Note that pyruvate is included in the following pathways: (i) TCA, (ii) glyoxylate metabolism, (iv) pyruvate metabolism, (v) Ala/Asp/Glu metabolism, and (vi) glycolysis.

LDH inhibition improves bone architecture and increases bone formation in mice

To further evaluate the effect of OXA on bone, we performed micro-CT analysis of mouse bones. We did not detect any significant differences between PBS- and OXA-treated groups in the spine (L5 & L6 levels, not shown). However, micro-CT of the femur revealed higher BMD of trabecular bone and increased cortical area and Polar Moment of Inertia (PMOI),

which reflects the bone geometry contribution to the resistance to torsional deformations (Fig. 5). Since both mineralization and appositional growth of cortical bone are functions of osteoblasts, these effects can be attributed to increased osteoblast activity. We therefore assessed osteoblast bone-forming function using dynamic bone histomorphometry and calcein double labeling (Fig. 6A). This analysis showed that OXA treatment of mice led to a significant increase in the mineral apposition rate (MAR) and bone formation rate (BFR) in the endocortical compartment (Fig. 6B – D), while periosteal and trabecular bone formation was not significantly changed (not shown). This data is consistent with the micro-CT data showing that OXA treatment mostly affected cortical region and to a lesser extent trabecular bone. This may also explain why the spine was not affected, because trabecular bone is the major component of the vertebrae.

We also measured bone resorption using osteoclast-specific TRAP staining (Fig. 6E) and Visiopharm technology-based automated histomorphometry. Figure 6F shows that TRAP staining and thus bone resorption was not significantly affected in OXA-treated mice when compared to the PBS-treated controls.

These assays demonstrate that OXA stimulates osteoblast bone-forming activity without affecting bone resorption leading to improved bone architecture in mice.

LDH inhibition increases bone strength in mice

Next, we investigated whether the observed bone anabolic effect of OXA leads to changes in bone biomechanical properties. We performed femur torsional testing, which revealed significant increases in maximum torque, maximal rotation, and energy to yield, compared to control PBS treated mice (Fig. 7).

Therefore, LDH inhibitor OXA significantly improves biomechanical strength of long bones in mice by increasing cortical bone area via endosteal appositional bone formation, independent of remodeling.

LDH inhibition exerts bone-anabolic effect in aged mice

The data presented above strongly indicate bone-anabolic effect of OXA in young mice. However, in healthy individuals bone loss is primarily associated with aging. We therefore tested whether OXA is effective against bone loss in aged mice. Eighteen-month-old male mice were subjected to the same OXA or vehicle regimen as young mice and analyzed with micro-CT after two months of treatment. Figure 8A shows that OXA treatment significantly improved femur trabecular bone to total volume (BV/TV) and trabecular thickness (Tb Th). In the cortical compartment (Fig. 8B), OXA significantly improved cortical thickness (Cort Th), area (Cort Area), and mineral density (Cort BMD).

DISCUSSION

The results presented in this study demonstrate that inhibition of LDH with OXA stimulates mitochondrial OxPhos and promotes osteoblast differentiation of C3H10T1/2 mouse osteoprogenitors and human BMSCs *in vitro*. Additionally, we observed that treating young and aged C57BL/6J male mice with OXA improved bone mineral density, trabecular and

cortical bone architecture, and bone biomechanical strength without causing organ toxicity. Furthermore, OXA treatment increased bone formation by osteoblasts without affecting osteoclast activity *in vivo*. Since we also observed the effect of OXA on fat tissue (Fig. 4), we cannot exclude the possibility that there is a systemic component of the effect on bone.

There is a growing body of literature describing the nuanced role of oxidative stress as a consequence of mitochondrial dysfunction in age-related bone disease.^(8,10) Previously, we reported a glycolytic shift following mitochondrial dysfunction in aged bone as a major contributor to bone loss in mice.⁽¹⁷⁾ As mitochondrial function declines, pathologic levels of intracellular ROS accumulate and the capacity for OxPhos, biosynthesis, and ion transport is impaired.^(43,44) In turn, ROS accumulation activates the mitochondrial permeability transition pore leading to mitochondrial swelling and a further decrease in ATP production.^(45,46) We have previously shown that protecting mitochondrial function by decreasing permeability transition pore sensitivity, using our cyclophilin D (CypD) knockout mouse model, results in a prevention of age-related bone loss and osteoporosis.⁽¹⁷⁾

As mitochondrial function is decreased while glycolysis is upregulated in aging bone, it is reasonable to assume that inhibiting the glycolytic shift would improve mitochondrial function. Before the extensive long-term aging study can be initiated, we had to perform a proof-of-concept study and find a safe way of inhibiting glycolysis. This strategy is being actively explored in anti-cancer therapies using inhibitors including 2DG, DCA, 3BP, and OXA known to shift energy metabolism from glycolysis to OxPhos.⁽⁴⁷⁾ Malignant cancer cells rely predominately on glycolysis, in contrast to their non-cancer counterparts which rely more heavily on mitochondrial OxPhos.⁽⁴⁸⁾

Current therapeutics for treating bone loss include bisphosphonates, which prevent excessive bone resorption by osteoclasts, and teriparatide, thereby promoting bone formation by osteoblasts. These drugs, however, are not without side effects and there remains a clinical need for additional agents that safely promote bone anabolism.^(49,50) Anti-glycolytic agents have been investigated for use in treating solid tumors, including liver, breast, pancreatic, brain, and lung cancers.^(35,51–56) The use of anti-glycolytic agents to improve bone quality has not been considered. As a consequence, their effects on bone are largely unknown. Our data demonstrate that of several glycolytic inhibitors used in this study, only OXA showed no significant toxicity *in vitro* after 48 h treatment. OXA is a pyruvate analog and competitive inhibitor of LDH, the metabolic enzyme that catalyzes the conversion of pyruvate into lactate and regenerates glycolytic NAD⁺. LDH expression is upregulated in cancer cells, and treatment with OXA has been shown to decrease lactate production and inhibit tumor progression.⁽⁵⁶⁾ OXA has also been used to investigate the mechanism of insulin resistance in type-2 diabetes. One study reported that lactate induces the transcription of pro-inflammatory cytokines, and that OXA treatment of adipose-like 3T3-L1 cells inhibits lactate production and improves insulin resistance.⁽⁵⁷⁾ A separate study reported that *in vitro* treatment of adipocytes with OXA caused an upregulation of intracellular lipolysis and significantly reduced triglyceride accumulation.⁽⁵⁸⁾ Furthermore, *db/db* mice treated with OXA had decreased lactate production in adipose and skeletal tissue and decreased body weight.⁽⁵⁹⁾ In our study, consistent with previous results, C57BL/6J mice treated with OXA showed decreased body fat percentage. However, we also observed a significant

increase in BMD. We observed that OXA treatment promoted cortical bone anabolism with minimal trabecular bone effects. An intriguing corollary to this observation; *in vivo* treatment of a glycolytic promoter teriparatide induced an increase in trabecular bone parameters, while having insignificant effects on cortical bone.⁽⁶⁰⁾ This suggests a possible metabolic difference between cortical and trabecular bone maintenance.

An interesting observation presented here is that the inhibitors of early steps of glycolysis, 2DG and 3BP, as well as a PDK inhibitor, DCA (Fig. 1A), were toxic to osteoprogenitors while the inhibitor of anaerobic glycolytic arm, OXA, was not. A possible explanation is that a glycolytic flux needs to be maintained in undifferentiated cells and all the tested inhibitors except for OXA are known to disrupt it. As an inhibitor of LDH-mediated fermentation arm of glycolysis, OXA does not disrupt the glycolytic flux but redirects it towards the TCA cycle. This finding demonstrates that when applied to normal non-cancerous cells and tissues, metabolic modifiers and inhibitors have to be carefully tested to avoid harmful side effects.

Our screen of bone metabolites following OXA treatment did not reveal significant changes in steady state lactate or pyruvate. However, as steady-state analysis cannot by definition provide information about metabolic flux it may be that OXA does induce changes in cell metabolism not captured by our detection method. Indeed the increase, though non-significant, in metabolite levels in glycolysis, pyruvate pathway, TCA cycle, and redox pathway could suggest an alteration in handling of these metabolites in the presence of OXA. Lastly, in our metabolomics study we observed only one metabolite with both significant p-value and fold change: Acetoacetyl-CoA. The metabolite is involved in ketone body synthesis as part of the HMG-CoA pathway. Interestingly this pathway has been implicated as an important link between obesity and osteoporosis and may warrant further investigation.⁽⁶¹⁾

While previous work has demonstrated the importance of mitochondrial metabolism for osteogenic differentiation and through genetic manipulation *in vivo*, to our knowledge this is the first study to consider use of an anti-glycolytic agent to promote bone anabolism. Since our study was a proof-of-principle, we studied this effect in male mice only to avoid confounding variables due to the protective effects of estrogen on mitochondria and OxPhos. Additional work is needed to include female mice to elucidate the effects of OXA on bone metabolism in the presence of estrogen. Studies of the effect of LDH inhibition in aged male and female mice will be most clinically relevant. We will also consider the use of other LDH inhibitors, including N-hydroxyindole (NHI-2), Gossypol, FX11, or galloflavin, as well as combination therapy. Lastly, while OXA treatment in mice was administered systemically, the outward appearance of the mice, including total bodyweight, were the same between the two groups and no systemic toxicity was observed in the OXA-treated mice. Even though systemic application did not cause visible side effects, the efficacy of the inhibitor may be further increased by designing bone-targeted derivatives in the future.

Overall, we demonstrate that inhibition of LDH with OXA leads to increased mitochondrial function and is an effective strategy to improve BMD, cortical bone architecture, and biomechanical properties in mice. The major limitations of our study were: i) the use of

male mice only; and ii) the use of 8-week-old and not aged mice. As this was done for the reasons specified above, future work will address these limitations as we now have a strong rationale to pursue a long-term study in both sexes. Our study implicates glycolytic metabolism as a novel therapeutic target for bone anabolism in age-related bone loss and osteoporosis.

Supplementary Material

Refer to Web version on PubMed Central for supplementary material.

ACKNOWLEDGEMENTS

We would like to thank Dr. Paul Brookes for the use of Seahorse apparatus, the histology core within the Center for Musculoskeletal Research (Kathy Maltby, Sarah Mack, and Jeffery Fox), the micro-CT core within the Center for Musculoskeletal Research (Michael Thullen) and biomechanics core (Emma Gira). Financial support was provided by NIH (R01 AR072601 and R21 AR07928 to R.A.E.; and R01 AR070613 and P30 AR069655- 5278 to H.A.) and by a grant to R.A.E. from the Orthopaedic Research and Education Foundation with additional funding provided by Musculoskeletal Transplant Foundation.

ABBREVIATIONS

BMSCs	Bone marrow stromal cells
OxPhos	oxidative phosphorylation
2DG	2-deoxyglucose
DCA	dichloroacetate
3-BP	3-bromopyruvate
OXA	sodium oxamate
PBS	phosphate-buffered saline
OCR	oxygen consumption rate
ECAR	extracellular acidification rate
Olig	oligomycin
FCCP	carbonyl cyanide p-trifluoromethoxyphenylhydrazine
AntA	antimycin A
Rot	rotenone
ALT	alanine aminotransferase
BMD	bone mineral density
DEXA	Dual Energy X-ray Absorptiometry
PMOI	polar moment of inertia

FFPE	formalin-fixed paraffin embedded
BFR	bone formation rate
TRAP	tartrate-resistant acid phosphatase
LDH	lactate dehydrogenase

REFERENCES

1. Bianco P, Cao X, Frenette PS, et al. The meaning, the sense and the significance: translating the science of mesenchymal stem cells into medicine. *Nature medicine*. 1 2013;19(1):35–42.
2. Vaananen HK, Laitala-Leinonen T. Osteoclast lineage and function. *Archives of biochemistry and biophysics*. 5 15 2008;473(2):132–8. [PubMed: 18424258]
3. Hwang ES, Yoon G, Kang HT. A comparative analysis of the cell biology of senescence and aging. *Cellular and molecular life sciences : CMLS*. 8 2009;66(15):2503–24. [PubMed: 19421842]
4. Lopez-Otin C, Blasco MA, Partridge L, Serrano M, Kroemer G. The hallmarks of aging. *Cell*. 6 6 2013;153(6):1194–217. [PubMed: 23746838]
5. Manolagas SC. Birth and death of bone cells: basic regulatory mechanisms and implications for the pathogenesis and treatment of osteoporosis. *Endocrine reviews*. 4 2000;21(2):115–37. [PubMed: 10782361]
6. Saito M, Marumo K. Bone quality in diabetes. *Frontiers in endocrinology*. 2013;4:72. [PubMed: 23785354]
7. Becerikli M, Jaurich H, Schira J, et al. Age-dependent alterations in osteoblast and osteoclast activity in human cancellous bone. *Journal of cellular and molecular medicine*. 11 2017;21(11):2773–81. [PubMed: 28444839]
8. Manolagas SC. From estrogen-centric to aging and oxidative stress: a revised perspective of the pathogenesis of osteoporosis. *Endocrine reviews*. 6 2010;31(3):266–300. [PubMed: 20051526]
9. Almeida M, Ambrogini E, Han L, Manolagas SC, Jilka RL. Increased lipid oxidation causes oxidative stress, increased peroxisome proliferator-activated receptor-gamma expression, and diminished pro-osteogenic Wnt signaling in the skeleton. *The Journal of biological chemistry*. 10 2 2009;284(40):27438–48. [PubMed: 19657144]
10. Lane RK, Hilsabeck T, Rea SL. The role of mitochondrial dysfunction in age-related diseases. *Biochimica et biophysica acta*. 11 2015;1847(11):1387–400. [PubMed: 26050974]
11. Eliseev RA, Filippov G, Velos J, et al. Role of cyclophilin D in the resistance of brain mitochondria to the permeability transition. *Neurobiology of aging*. 10 2007;28(10):1532–42. [PubMed: 16876914]
12. Nunomura A, Castellani RJ, Zhu X, Moreira PI, Perry G, Smith MA. Involvement of oxidative stress in Alzheimer disease. *Journal of neuropathology and experimental neurology*. 7 2006;65(7):631–41. [PubMed: 16825950]
13. McManus MJ, Murphy MP, Franklin JL. Mitochondria-derived reactive oxygen species mediate caspase-dependent and -independent neuronal deaths. *Molecular and cellular neurosciences*. 11 2014;63:13–23. [PubMed: 25239010]
14. Santos D, Esteves AR, Silva DF, Januario C, Cardoso SM. The Impact of Mitochondrial Fusion and Fission Modulation in Sporadic Parkinson's Disease. *Molecular neurobiology*. 8 2015;52(1):573–86. [PubMed: 25218511]
15. Figueiredo PA, Powers SK, Ferreira RM, Appell HJ, Duarte JA. Aging impairs skeletal muscle mitochondrial bioenergetic function. *The journals of gerontology Series A, Biological sciences and medical sciences*. 1 2009;64(1):21–33.
16. Harrison CM, Pompilius M, Pinkerton KE, Ballinger SW. Mitochondrial oxidative stress significantly influences atherogenic risk and cytokine-induced oxidant production. *Environmental health perspectives*. 5 2011;119(5):676–81. [PubMed: 21169125]

17. Shum LC, White NS, Nadtochiy SM, et al. Cyclophilin D Knock-Out Mice Show Enhanced Resistance to Osteoporosis and to Metabolic Changes Observed in Aging Bone. *PLoS one*. 2016;11(5):e0155709. [PubMed: 27183225]
18. Baker N, Boyette LB, Tuan RS. Characterization of bone marrow-derived mesenchymal stem cells in aging. *Bone*. 1 2015;70:37–47. [PubMed: 25445445]
19. Shum LC, White NS, Mills BN, Bentley KL, Eliseev RA. Energy Metabolism in Mesenchymal Stem Cells During Osteogenic Differentiation. *Stem cells and development*. 1 15 2016;25(2):114–22. [PubMed: 26487485]
20. Varum S, Rodrigues AS, Moura MB, et al. Energy metabolism in human pluripotent stem cells and their differentiated counterparts. *PLoS one*. 2011;6(6):e20914. [PubMed: 21698063]
21. Chen CT, Shih YR, Kuo TK, Lee OK, Wei YH. Coordinated changes of mitochondrial biogenesis and antioxidant enzymes during osteogenic differentiation of human mesenchymal stem cells. *Stem cells (Dayton, Ohio)*. 4 2008;26(4):960–8.
22. Guntur AR, Le PT, Farber CR, Rosen CJ. Bioenergetics during calvarial osteoblast differentiation reflect strain differences in bone mass. *Endocrinology*. 5 2014;155(5):1589–95. [PubMed: 24437492]
23. Pattappa G, Heywood HK, de Bruijn JD, Lee DA. The metabolism of human mesenchymal stem cells during proliferation and differentiation. *Journal of cellular physiology*. 10 2011;226(10):2562–70. [PubMed: 21792913]
24. Esen E, Chen J, Karner CM, Okunade AL, Patterson BW, Long F. WNT-LRP5 signaling induces Warburg effect through mTORC2 activation during osteoblast differentiation. *Cell metabolism*. 5 7 2013;17(5):745–55. [PubMed: 23623748]
25. Intlekofer AM, Finley LWS. Metabolic signatures of cancer cells and stem cells. *Nature metabolism*. 2 2019;1(2):177–88.
26. Shin MK, Cheong JH. Mitochondria-centric bioenergetic characteristics in cancer stem-like cells. *Archives of pharmacological research*. 2 2019;42(2):113–27. [PubMed: 30771209]
27. Seo BJ, Yoon SH, Do JT. Mitochondrial Dynamics in Stem Cells and Differentiation. *International journal of molecular sciences*. 12 5 2018;19(12).
28. Luengo A, Gui DY, Vander Heiden MG. Targeting Metabolism for Cancer Therapy. *Cell chemical biology*. 9 21 2017;24(9):1161–80. [PubMed: 28938091]
29. Zhu J, Zheng Y, Zhang H, Sun H. Targeting cancer cell metabolism: The combination of metformin and 2-Deoxyglucose regulates apoptosis in ovarian cancer cells via p38 MAPK/JNK signaling pathway. *American journal of translational research*. 2016;8(11):4812–21. [PubMed: 27904682]
30. Zhao Z, Han F, Yang S, Wu J, Zhan W. Oxamate-mediated inhibition of lactate dehydrogenase induces protective autophagy in gastric cancer cells: involvement of the Akt-mTOR signaling pathway. *Cancer letters*. 3 1 2015;358(1):17–26. [PubMed: 25524555]
31. Miskimins WK, Ahn HJ, Kim JY, Ryu S, Jung YS, Choi JY. Synergistic anti-cancer effect of phenformin and oxamate. *PLoS one*. 2014;9(1):e85576. [PubMed: 24465604]
32. Shares BH, Busch M, White N, Shum L, Eliseev RA. Active mitochondria support osteogenic differentiation by stimulating β -catenin acetylation. *The Journal of biological chemistry*. 10 12 2018;293(41):16019–27. [PubMed: 30150300]
33. Smith CO, Wang YT, Nadtochiy SM, et al. Cardiac metabolic effects of KNa1.2 channel deletion and evidence for its mitochondrial localization. *FASEB journal : official publication of the Federation of American Societies for Experimental Biology*. 6 4 2018:fj201800139R.
34. Xia J, Wishart DS. Using MetaboAnalyst 3.0 for Comprehensive Metabolomics Data Analysis. *Current protocols in bioinformatics*. 9 7 2016;55:14.0.1–.0.91.
35. Yang Y, Su D, Zhao L, et al. Different effects of LDH-A inhibition by oxamate in non-small cell lung cancer cells. *Oncotarget*. 12 15 2014;5(23):11886–96. [PubMed: 25361010]
36. Forni MF, Peloggia J, Trudeau K, Shirihai O, Kowaltowski AJ. Murine Mesenchymal Stem Cell Commitment to Differentiation Is Regulated by Mitochondrial Dynamics. *Stem cells (Dayton, Ohio)*. 3 2016;34(3):743–55.

37. Caslin HL, Taruselli MT, Haque T, et al. Inhibiting Glycolysis and ATP Production Attenuates IL-33-Mediated Mast Cell Function and Peritonitis. *Frontiers in immunology*. 2018;9:3026. [PubMed: 30619366]
38. Hughes DE, Dai A, Tiffée JC, Li HH, Mundy GR, Boyce BF. Estrogen promotes apoptosis of murine osteoclasts mediated by TGF-beta. *Nature medicine*. 10 1996;2(10):1132–6.
39. Qu Q, Perala-Heape M, Kapanen A, et al. Estrogen enhances differentiation of osteoblasts in mouse bone marrow culture. *Bone*. 3 1998;22(3):201–9. [PubMed: 9514212]
40. Ernst M, Schmid C, Froesch ER. Enhanced osteoblast proliferation and collagen gene expression by estradiol. *Proceedings of the National Academy of Sciences of the United States of America*. 4 1988;85(7):2307–10. [PubMed: 3353379]
41. Riggs BL, Khosla S, Melton LJ 3rd. Sex steroids and the construction and conservation of the adult skeleton. *Endocrine reviews*. 6 2002;23(3):279–302. [PubMed: 12050121]
42. Brand MD, Nicholls DG. Assessing mitochondrial dysfunction in cells. *The Biochemical journal*. 4 15 2011;435(2):297–312. [PubMed: 21726199]
43. Lu T, Finkel T. Free radicals and senescence. *Experimental cell research*. 6 10 2008;314(9):1918–22. [PubMed: 18282568]
44. Giorgio M, Migliaccio E, Orsini F, et al. Electron transfer between cytochrome c and p66Shc generates reactive oxygen species that trigger mitochondrial apoptosis. *Cell*. 7 29 2005;122(2):221–33. [PubMed: 16051147]
45. Almeida M, Han L, Ambrogini E, Bartell SM, Manolagas SC. Oxidative stress stimulates apoptosis and activates NF-kappaB in osteoblastic cells via a PKCbeta/p66shc signaling cascade: counter regulation by estrogens or androgens. *Molecular endocrinology (Baltimore, Md)*. 10 2010;24(10):2030–7.
46. Almeida M, Han L, Martin-Millan M, et al. Skeletal involution by age-associated oxidative stress and its acceleration by loss of sex steroids. *The Journal of biological chemistry*. 9 14 2007;282(37):27285–97. [PubMed: 17623659]
47. Abdel-Wahab AF, Mahmoud W, Al-Harizy RM. Targeting glucose metabolism to suppress cancer progression: prospective of anti-glycolytic cancer therapy. *Pharmacological research*. 12 2019;150:104511. [PubMed: 31678210]
48. Granchi C, Minutolo F. Anticancer agents that counteract tumor glycolysis. *ChemMedChem*. 8 2012;7(8):1318–50. [PubMed: 22684868]
49. Kennel KA, Drake MT. Adverse effects of bisphosphonates: implications for osteoporosis management. *Mayo Clinic proceedings*. 7 2009;84(7):632–7; quiz 8. [PubMed: 19567717]
50. Stroup J, Kane MP, Abu-Baker AM. Teriparatide in the treatment of osteoporosis. *American journal of health-system pharmacy : AJHP : official journal of the American Society of Health-System Pharmacists*. 3 15 2008;65(6):532–9. [PubMed: 18319498]
51. Jae HJ, Chung JW, Park HS, et al. The antitumor effect and hepatotoxicity of a hexokinase II inhibitor 3-bromopyruvate: in vivo investigation of intraarterial administration in a rabbit VX2 hepatoma model. *Korean journal of radiology*. 11-12 2009;10(6):596–603. [PubMed: 19885316]
52. Xu D, Jin J, Yu H, et al. Chrysin inhibited tumor glycolysis and induced apoptosis in hepatocellular carcinoma by targeting hexokinase-2. *Journal of experimental & clinical cancer research : CR*. 3 20 2017;36(1):44. [PubMed: 28320429]
53. Tao L, Wei L, Liu Y, et al. Gen-27, a newly synthesized flavonoid, inhibits glycolysis and induces cell apoptosis via suppression of hexokinase II in human breast cancer cells. *Biochemical pharmacology*. 2 1 2017;125:12–25. [PubMed: 27818240]
54. Coleman MC, Asbury CR, Daniels D, et al. 2-deoxy-D-glucose causes cytotoxicity, oxidative stress, and radiosensitization in pancreatic cancer. *Free radical biology & medicine*. 2 1 2008;44(3):322–31. [PubMed: 18215740]
55. Dunbar EM, Coats BS, Shroads AL, et al. Phase 1 trial of dichloroacetate (DCA) in adults with recurrent malignant brain tumors. *Investigational new drugs*. 6 2014;32(3):452–64. [PubMed: 24297161]
56. Le A, Cooper CR, Gouw AM, et al. Inhibition of lactate dehydrogenase A induces oxidative stress and inhibits tumor progression. *Proceedings of the National Academy of Sciences of the United States of America*. 2 2 2010;107(5):2037–42. [PubMed: 20133848]

57. Samuvel DJ, Sundararaj KP, Nareika A, Lopes-Virella MF, Huang Y. Lactate boosts TLR4 signaling and NF-kappaB pathway-mediated gene transcription in macrophages via monocarboxylate transporters and MD-2 up-regulation. *Journal of immunology (Baltimore, Md : 1950)*. 2 15 2009;182(4):2476–84.
58. Si Y, Shi H, Lee K. Impact of perturbed pyruvate metabolism on adipocyte triglyceride accumulation. *Metabolic engineering*. 11 2009;11(6):382–90. [PubMed: 19683593]
59. Ye W, Zheng Y, Zhang S, Yan L, Cheng H, Wu M. Oxamate Improves Glycemic Control and Insulin Sensitivity via Inhibition of Tissue Lactate Production in db/db Mice. *PloS one*. 2016;11(3):e0150303. [PubMed: 26938239]
60. Esen E, Lee SY, Wice BM, Long F. PTH Promotes Bone Anabolism by Stimulating Aerobic Glycolysis via IGF Signaling. *Journal of bone and mineral research : the official journal of the American Society for Bone and Mineral Research*. 11 2015;30(11):1959–68.
61. Yamasaki M, Hasegawa S, Imai M, Takahashi N, Fukui T. High-fat diet-induced obesity stimulates ketone body utilization in osteoclasts of the mouse bone. *Biochemical and biophysical research communications*. 4 29 2016;473(2):654–61. [PubMed: 27021680]

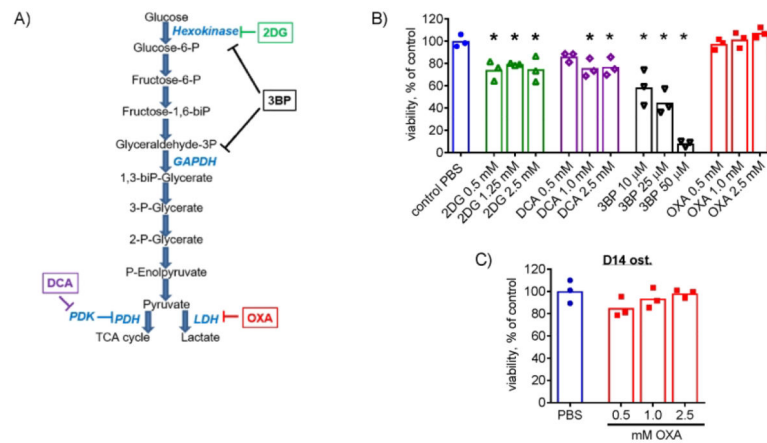


Figure 1. Effect of various anti-glycolytic agents on osteoprogenitors.

(A) Anti-glycolytic agents including 2-deoxyglucose (2DG), dichloroacetate (DCA), 3-bromopyruvate (3-BP), and sodium oxamate (OXA) were used to target various steps of the glycolytic pathway. (B) Undifferentiated C3H10T1/2 cells were treated with PBS as a vehicle control or various indicated doses of 2DG, DCA, 3-BP, or OXA for 48 h. Cells were then stained with Calcein AM at 1 μ M for 30 min to assess viability. Only OXA did not cause any toxicity at the studied concentrations. (C) C3H10T1/2 cells were osteoinduced for 14 days in medium containing ascorbic acid and β -glycerol phosphate and then treated with OXA for 48 h. Calcein AM staining revealed no significant negative effect of OXA on the viability of osteoinduced C3H10T1/2 cells. Data are presented as boxplots with actual data points, median, and range. *P* value was determined by ANOVA shown in data sets with *p* < 0.05.

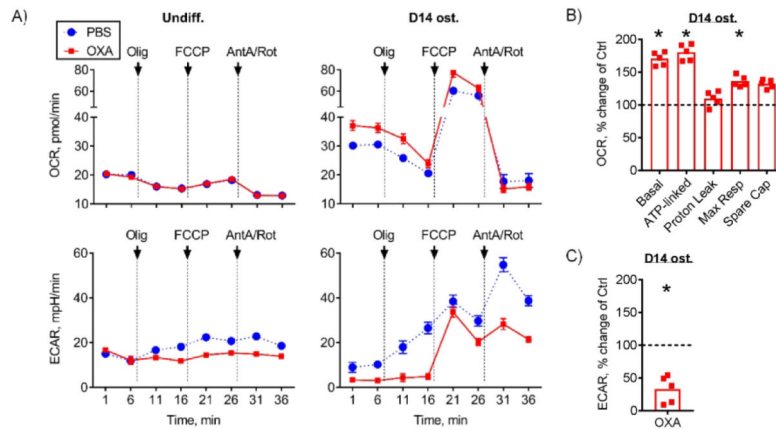


Figure 2. LDH inhibitor oxamate diverts cell bioenergetics from glycolysis to oxidative phosphorylation.

Bioenergetic profiling of undifferentiated and osteoinduced C3H10T1/2 cells in the presence of 1 mM OXA or PBS using Seahorse XF96. Oxygen consumption rate (OCR) measures OxPhos activity and extracellular acidification rate (ECAR) measures glycolytic activity. (A) OCR and ECAR measurements were taken at baseline and after addition of Olig (Oligomycin A, inhibitor of mitochondrial ATP-Synthase), FCCP (Carbonyl cyanide-p-trifluoromethoxyphenylhydrazone, protonophore which uncouples mitochondrial proton gradient), and AntA/Rot (Antimycin A and Rotenone, inhibitors of mitochondrial electron transport chain complexes III and I respectively). Undifferentiated cells have minimal reliance on OxPhos and treatment with OXA had no effect on OxPhos or basal glycolytic activity (left panel). In osteoinduced C3H10T1/2 cells, OXA treatment led to inhibition of glycolysis and further activation of OxPhos (right panel). Osteoinduced C3H10T1/2 cells treated with OXA had (B) significantly increased OCR values, including basal, ATP-linked, and maximal respiration, and (C) significantly reduced ECAR values. This demonstrates that OXA stimulates OxPhos and inhibits glycolysis in osteoinduced cells. Data are presented as boxplots with actual data points, median, and range. P value was determined by unpaired t -test and shown in data sets with $p < 0.05$.

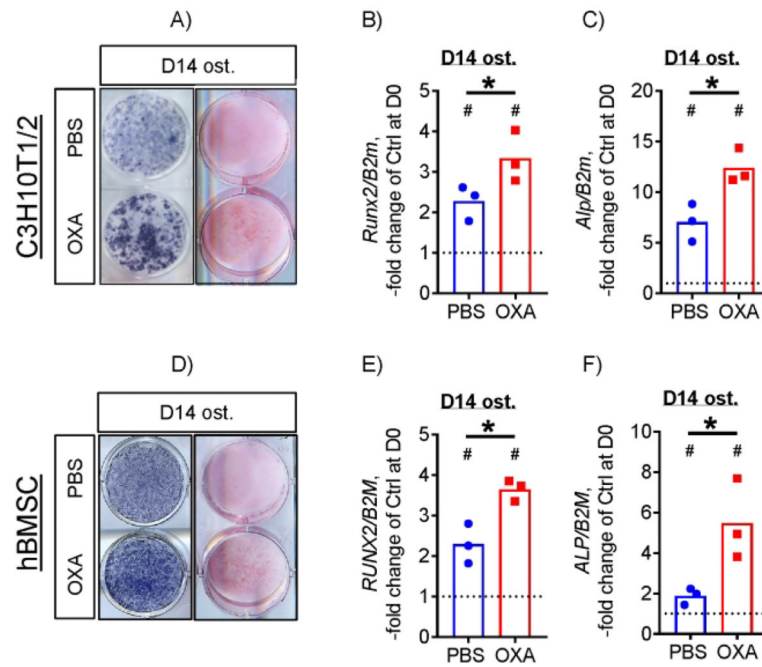


Figure 3. LDH inhibition increases osteogenic potential of both mouse and human osteoprogenitors.

C3H10T1/2 cells osteoinduced for 14 days in the presence of 1 mM OXA show increased ALP (A, left column) and Alizarin Red (A, right column) staining and expression of osteogenic markers *Runx2* (B) and *Alp* (C). Human BMSCs osteoinduced for 14 days in the presence of 1 mM OXA show higher levels of ALP (A, left column) and Alizarin Red (A, right column) staining and *RUNX2* (E) and *ALP* (F) expression. Images are representative of 6 (3 independent batches of cells, 2 technical replicates). Data are presented as boxplots with actual data points, median, and range. *P* value of D14 vs D0 (vertical text) or OXA vs PBS (horizontal text) was determined by unpaired *t*-test and shown in data sets with $p < 0.05$.

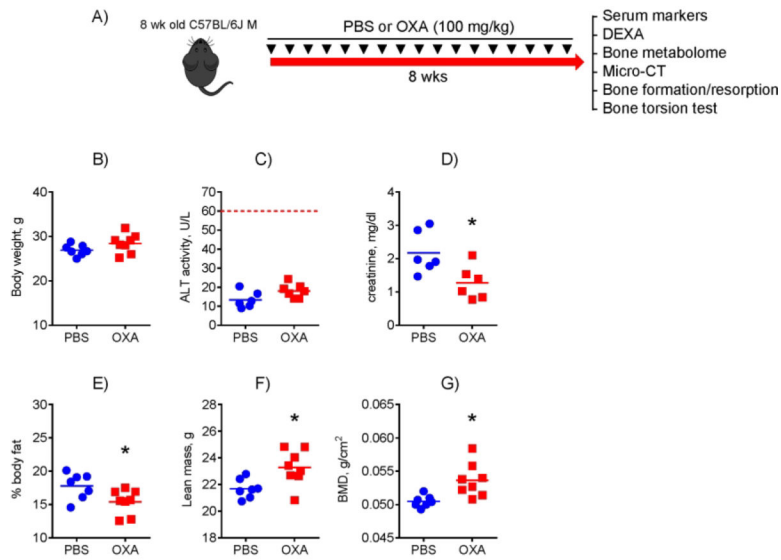


Figure 4. Mice treated with LDH inhibitor oxamate have increased bone mineral density without any signs of toxicity.

A) Eight-week-old male C57BL/6J mice were treated with 100 mg/kg OXA or PBS twice per week for 2 mo and tissues were collected for various analyses. OXA toxicity was assessed and compared to PBS-treated controls: (B) Body weight; (C) serum ALT (liver toxicity); (D) serum creatinine (kidney marker). Whole body composition was measured via DEXA: (E) % body fat; (F) Lean mass; (G) Bone mineral density (BMD). Data are presented as boxplots with actual data points, median, and range. P value was determined by unpaired t -test and shown in data sets with $p < 0.05$.

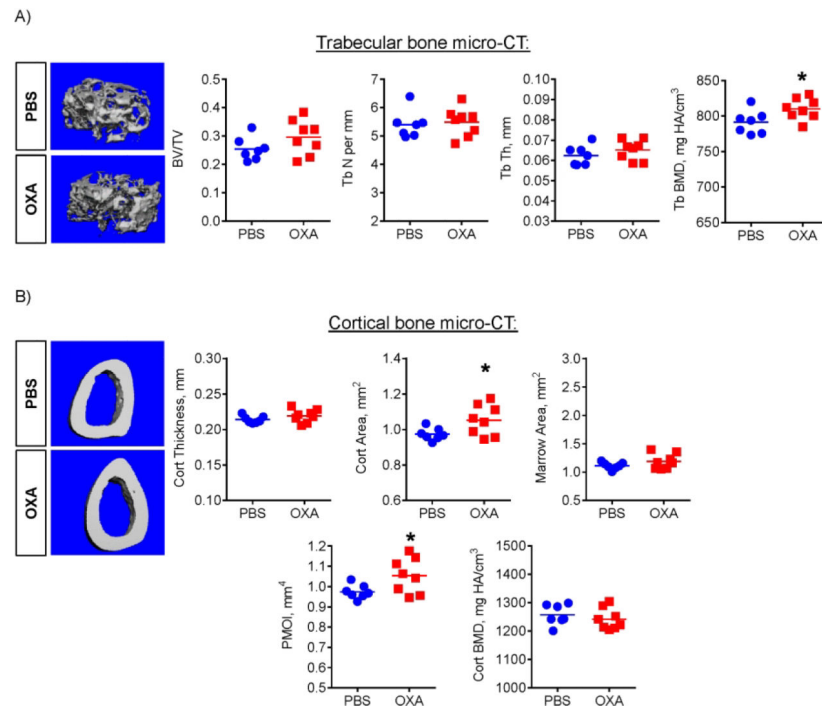


Figure 5. LDH inhibition improves trabecular bone density and cortical bone architecture in mice.

Effect of OXA on femur bone architecture, as analyzed by micro-CT. OXA-treated mice showed increased (A) trabecular bone mineral density (BMD) and (B) cortical area and polar moment of inertia (PMOI). Data are presented as boxplots with actual data points, median, and range. *P* value was determined by unpaired *t*-test and shown in data sets with *p* < 0.05.

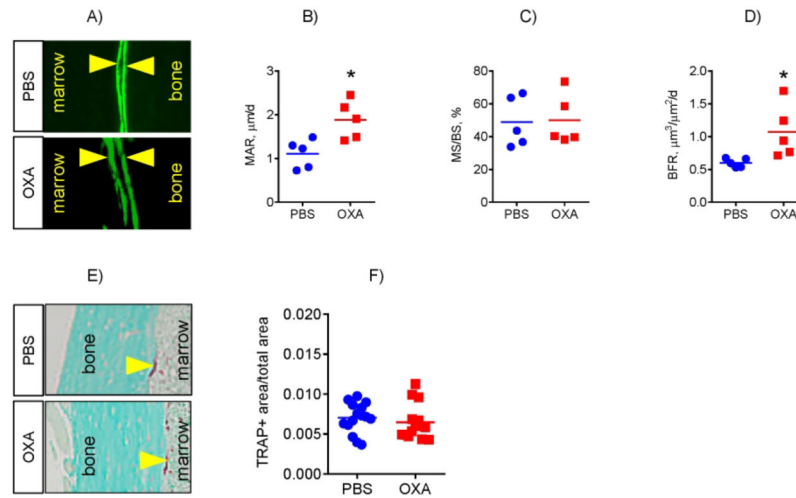


Figure 6. LDH inhibition stimulates osteoblast bone forming activity without affecting bone resorption in mice.

(A) Analysis of osteoblast bone forming function using dynamic bone histomorphometry and calcein double labeling. (B – D) OXA treatment of mice led to a significant increase in mineral apposition rate (MAR) and bone formation rate (BFR) in the endocortical compartment of femoral bone. (E) Analysis of osteoclast-specific TRAP staining and Visiopharm technology-based automated histomorphometry. (F) Bone resorption was not significantly affected in OXA-treated mice when compared to PBS-treated controls. Data are presented as boxplots with actual data points, median, and range. *P* value was determined by unpaired *t*-test and shown in data sets with $p < 0.05$.

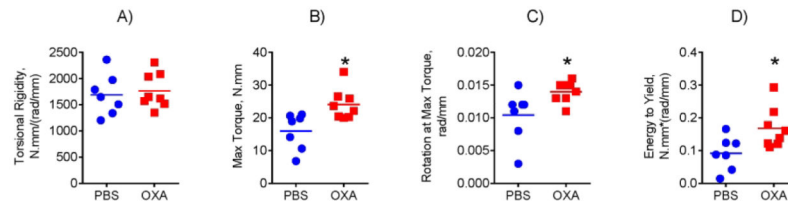


Figure 7: LDH inhibition increases bone strength in mice.

Biomechanical properties of mice after treatment with OXA or PBS were assessed via femoral torsion testing. OXA-treated mice revealed (A) no change in torsional rigidity, but showed significant increases in (B) maximum torque, (C) maximal rotation, and (D) energy to yield. Data are presented as boxplots with actual data points, median, and range. P value was determined by unpaired t -test and shown in data sets with $p < 0.05$.

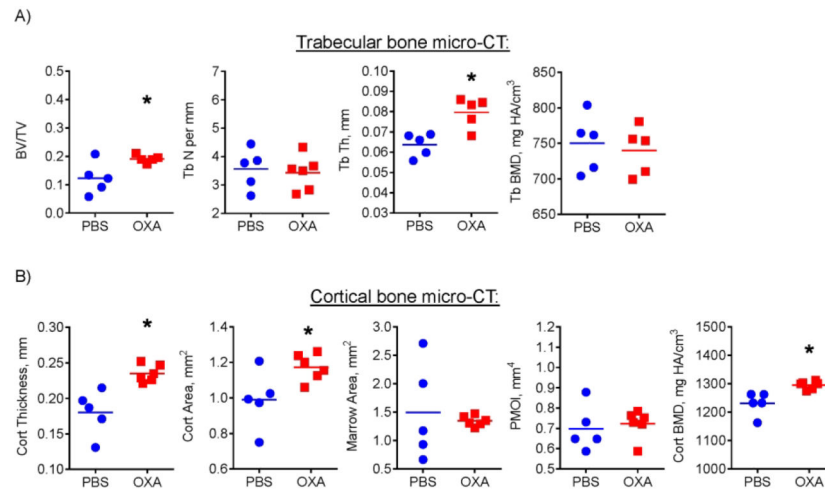


Figure 8. LDH inhibition improves trabecular and cortical bone in aged mice.

Effect of OXA on femur bone architecture was analyzed by micro-CT. OXA-treated mice showed increased (A) trabecular bone to total volume ratio and trabecular thickness and (B) cortical thickness, area, and bone mineral density (BMD). Data are presented as boxplots with actual data points, median, and range. *P* value was determined by unpaired *t*-test and shown in data sets with $p < 0.05$.